Vol. 276: 37–51, 2004 | MARINE ECOLOGY PROGRESS SERIES
Mar Ecol Prog Ser | Published August 2

Anoxic nitrification in marine sediments

Robert J. G. Mortimer[1,*], Sansha J. Harris[1], Michael D. Krom[1], Thomas E. Freitag[2], James I. Prosser[2], Jonathan Barnes[3], Pierre Anschutz[4], Peter J. Hayes[5], Ian M. Davies[5]

[1]Earth and Biosphere Institute, School of Earth Sciences, University of Leeds, Leeds LS2 9JT, UK

[2]Department of Molecular & Cell Biology, University of Aberdeen, Institute of Medical Sciences, Foresterhill, Aberdeen AB25 2ZD, UK

[3]Department of Marine Sciences and Coastal Management, University of Newcastle-upon-Tyne, Newcastle, UK

[4]Université Bordeaux 1, Departement de Geologie et Oceanographie (D.G.O.), CNRS UMR 5805, 33405 Talence Cedex, France

[5]Fisheries Research Services, Marine Laboratory, Aberdeen AB11 9DB, UK

ABSTRACT: Nitrate peaks are found in pore-water profiles in marine sediments at depths considerably below the conventional zone of oxic nitrification. These have been interpreted to represent non-steady-state effects produced by the activity of nitrifying bacteria, and suggest that nitrification occurs throughout the anoxic sediment region. In this study, ΣNO3 peaks and molecular analysis of DNA and RNA extracted from anoxic sediments of Loch Duich, an organic-rich marine fjord, are consistent with nitrification occurring in the anoxic zone. Analysis of ammonia oxidiser 16S rRNA gene fragments amplified from sediment DNA indicated the abundance of autotrophic ammonia-oxidising bacteria throughout the sediment depth sampled (40 cm), while RT-PCR analysis indicated their potential activity throughout this region. A large non-steady-state pore-water ΣNO3 peak at ~21 cm correlated with discontinuities in this ammonia-oxidiser community. In addition, a subsurface nitrate peak at ~8 cm below the oxygen penetration depth, correlated with the depth of a peak in nitrification rate, assessed by transformation of ^{15}N-labelled ammonia. The source of the oxidant required to support nitrification within the anoxic region is uncertain. It is suggested that rapid recycling of N is occurring, based on a coupled reaction involving Mn oxides (or possibly highly labile Fe oxides) buried during small-scale slumping events. However, to fully investigate this coupling, advances in the capability of high-resolution pore-water techniques are required.

KEY WORDS: Anoxic nitrification · Diffusive Equilibrium in Thin films (DET) · 16sRNA

INTRODUCTION

Nitrification is the microbial oxidation of ammonia to nitrite and then to nitrate; a 2 step process performed by distinct chemoautotrophic bacterial populations, the ammonia-oxidising bacteria (AOB) and the nitrite-oxidising bacteria respectively (Warrington 1878, Winogradsky 1891). Because of the use of oxygen as terminal electron acceptor, nitrification is traditionally considered to be restricted to aerobic environments (e.g. Froelich et al. 1979). According to this model, nitrate production through nitrification will only occur within the uppermost oxic layers of marine sediments. Below the oxic layer, the concentration of nitrate decreases, as it is used as a terminal electron acceptor by heterotrophic nitrate reducing bacteria (Froelich et al. 1979). Consequently, typical profiles of nitrate in recent marine sediments show maximum concentrations at the oxic/anoxic interface, followed by an exponential decrease with increasing depth (e.g. Fenchel et al. 1998). However, bacteria of the phylum Planctomycetes have recently been demonstrated to oxidise ammonia with nitrite as terminal electron acceptor under anoxic conditions (the 'anammox' process, Jetten et al. 1997), and physiological studies on *Nitrosomonas europaea* and *N. eutropha* suggest that the

*Email: r.mortimer@earth.leeds.ac.uk

anaerobic oxidation of ammonia may also be carried out by β-proteobacterial ammonia oxidising bacteria (Schmidt & Bock 1997, 1998). Recent work has suggested that ammonium oxidation coupled to the reduction of manganese ('anoxic nitrification') may occur in continental shelf sediments (Luther et al. 1997, 1998, Mortimer & Krom 1998, Mortimer et al. 1998, Hulth et al. 1999, Anschutz et al. 2000, Hyacinthe et al. 2001, Deflandre et al. 2002, Mortimer et al. 2002).

Field evidence suggests that anammox is a significant process, accounting for up to 50% of N_2 production in the marine environment (Thamdrup & Dalsgaard 2002, Dalsgaard et al. 2003, Kuypers et al. 2003). In contrast, the importance of anoxic nitrification is the subject of debate. Luther et al. (1997) calculated that this reaction might account for 90% of N_2 formation in continental margin, whereas Thamdrup & Dalsgaard (2000) found it to be an insignificant process in Mn-rich sediments of the Skagerrak. Anoxic nitrification is difficult to measure, particularly *in situ*, and hence more work is required to quantify its global significance.

In general, evidence for the existence of anoxic nitrification pathways in marine sediments has been provided by geochemical data, including profiles of pore-water and solid-phase constituents (e.g. Anschutz et al. 2000, Hyacinthe et al. 2001, Deflandre et al. 2002, Mortimer et al. 2002), laboratory incubations (Hulth et al. 1999), and thermodynamic calculations (Luther et al. 1997, 1998). To date, no study investigating anoxic nitrification in marine sediments has attempted to support geochemical data by microbiological analysis.

Recently Mortimer & Krom (1998) and Mortimer et al. (1998, 2002) analysed pore-waters within sediments from an organic-rich marine fjord by applying the high-resolution 'diffusive equilibrium in thin films' (DET) gel technology, and demonstrated the presence of a ΣNO_3 peak deep within the anoxic region. The authors argued that this peak was not caused by bioturbation because: (1) a ΣNO_3 peak was also evident at a comparable depth in conventional pore-water samples taken from the same box core, despite the fact that these samples were horizontally separated by several centimetres and it is extremely unlikely that a burrow would have intersected both samples at the same depth; (2) there was no minimum in the ammonia profile measured by DET, which would be expected if macrofauna introduced enough oxygen to trigger conventional nitrification at depth (cf. Mortimer et al. 1999); and (3) there were no changes in redox-sensitive species. The authors therefore suggested that this ΣNO_3 peak represented evidence of anoxic nitrification.

In this study, we revisited the same sampling site, and used DET gel technology and conventional interstitial water analyses to characterise possible anoxic nitrification. Problems that may previously have given poor detection limits for nitrate in saline waters by ion chromatography (IC), have been overcome by using a micro-nitrate Cd/Cu method capable of measuring ΣNO_3 in 100 µl samples (Harris & Mortimer 2002). In addition, molecular methods were used to characterise microbial populations, and nitrification rates were determined using ^{15}N-based techniques. For molecular analysis of ammonia oxidising communities, we used 16S rRNA gene primers semi-specific for bacteria of the phylum *Planctomycetes* and specific for β-proteobacterial ammonia oxidisers. PCR products were analysed by denaturing gradient gel electrophoresis (DGGE) and sequencing of excised DGGE bands, followed by phylogenetic analysis. Molecular characterisation eliminates the requirement for laboratory cultivation, a major limitation of traditional methods for analysis of bacterial community structure. Analysis of RNA provides greater sensitivity, through higher target copy number, and in comparison to analysis of DNA may indicate which members of the community are more metabolically active, since active cells have a higher ribosomal content (Wagner et al. 1995, Kowalchuk et al. 1999).

Conventional methods of determining nitrification rates *in situ* rely on the use of a ^{15}N stable isotope as a tracer followed by recovery of labelled end products (e.g. nitrate). Determination of the ^{15}N content of the nitrate pool requires reduction, followed by recovery as the ammonium salt, before conversion to N_2 and analysis by isotope ratio mass spectroscopy (IRMS). Such methods are not only time-consuming, but also subject to isotopic dilution and cross-contamination. In this study, we used a new technique based on determining ^{15}N in nitrate and nitrite by conversion to nitrous oxide (Stevens & Laughlin 1994). This method enables assessment of nitrification and nitrous oxide production in sediment cores after addition of $^{15}NH_4^+$ while obviating the need for distillation or diffusion, and the short incubation period employed facilitates comparison with true environmental conditions.

Together, geochemical and molecular analysis were carried out (1) to determine the geochemical evidence for anoxic nitrification, (2) to characterise the microbial communities of nitrifying bacteria present in the anoxic sediments sampled, and (3) to determine whether the population was potentially active.

MATERIALS AND METHODS

Sampling location. The sediments studied were collected from 120 m water depth in the centre of Loch Duich, an organic-rich marine fjord on the west coast of Scotland (Site RM1, Fig. 1).

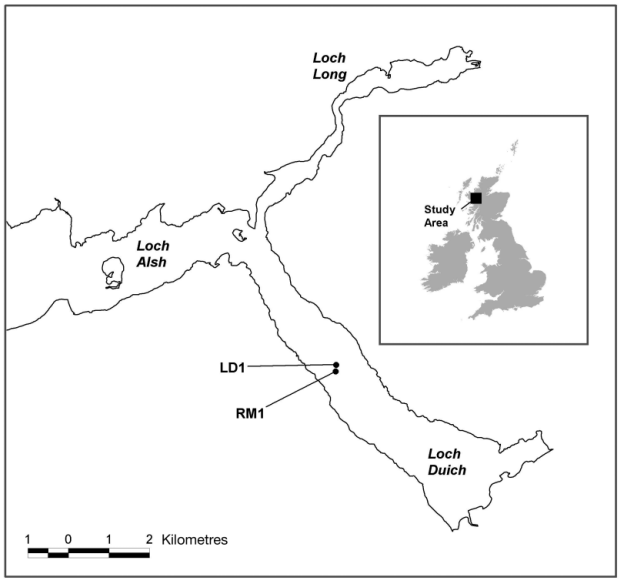

Fig. 1. Study area. LD1, RM1: sites of cores in the centre of Loch Duich, west coast of Scotland

Sample collection and sampling design. The sediments were collected in July 2000 on board FRV 'Clupea' using a stainless steel box corer of 0.35 × 0.35 × >1 m deep. Sampling with the box corer enabled preservation of the sediment structure, indicated by a clearly defined surface horizon comprising a brown oxic layer. The box core, allowed the concurrent deployment of several sampling techniques, but its limited dimensions prevented all methods of analysis on the same box core sediment. Therefore sampling was carried out in sets of 2, 3 or 4 within individual box cores from the same sampling site.

Pore-water sampling. Depth profiles of pore-water O_2 were measured on board using a cathode-type mini-electrode (Revsbech 1983) immediately after core recovery. We used a voltammetric gold amalgam mini-electrode (Brendel & Luther 1995) to determine depth profiles of dissolved sulphide and to confirm oxygen profiles. Comparing oxygen profiles obtained with both techniques showed excellent agreement. The construction of the voltammetric electrode and the measurements were carried out as described by Anschutz et al. (2000). Briefly, a standard 3-electrode voltammetric cell was used for all electrochemical measurements with the mini-electrode as working electrode, a 0.5 mm diameter platinum wire as counter electrode, and a Ag/AgCl as reference electrode. An Analytical Instrument Systems (AIS) model DLK-100 electrochemical analyser was used for all measurements. Oxygen was determined with linear sweep voltammetry (LSV), scanning from –0.1 V to –1.7 V at a rate of 200 mV s^{-1} after 10 s equilibration at –0.1 V. The detection limit at the 99% confidence limit for O_2 was 3 µM. Precision for replicates of all species at a given depth is typically 2–5%. The microelectrode profiling was carried out at the *in situ* temperature. Each vertical profile consisted of about 50 measurements, taking about 2 min each. Thus, all microelectrode measurements were completed within 2 h of sampling.

Conventional pore-water extractions were performed on sediment sub-cores of 10 cm diameter removed from Box Cores 8 and 9. All pore-water processing was completed on board under continuous nitrogen flow in a glove box. Sediment cores were sliced at 1 cm intervals for the first 10 cm, 2 cm for the next 10 cm and at 4 cm thereafter, and sediments stored in 125 ml bottles (Nalgene). Subsamples were placed in zip-lock bags and immediately stored at –20°C for porosity determination and at –70°C for molecular analysis. After processing the core, the Nalgene bottles were briefly removed from the glove box for centrifugation at 3000 rpm for 10 min to extract the pore-water, and returned immediately into the glove box. Supernatants from the bottles were then filtered (0.45 µm; Nuclepore) into 30 ml Nunc vials, from which aliquots were pipetted into pore-water storage vials pre-filled with the appropriate preservative (Table 1).

DET gel probes (Davison et al. 1994, Krom et al. 1994, Mortimer et al. 1998) were used to determine pore-water ΣNO_3 concentrations in Box Cores 7 and 9. Prior to deployment, the DET probes were conditioned in artificial seawater and deoxygenated by sparging with N_2 for 24 h. For Box Core 7, the DET gel probe was inserted into a 10 cm diameter sub-core that had been removed from the box core. For Box Core 9, the DET gel probe was inserted directly into the box core. Prior to probe deployment, surface seawater from Loch Duich was carefully introduced onto the surface of both the sub-core and box core in order to prevent artefacts caused by ingress of air at the sediment-water interface. The probes were left to equilibrate for 17 h before sampling using standard procedures (Mortimer et al.1998).

Analysis of pore-water and gel samples. The conventional pore-water samples were additionally analysed for a range of geochemical determinants to define the biogeochemical zonation of the sediments

Table 1. Volume of pore-waters extracted and preservatives used

Analysis	Vol. (ml)	Preservative
Sulphate and chloride	2	None
Sulphide	1	Diamine reagent
Iron and manganese	2	HNO_3

within which anoxic nitrification was occurring. Higher-resolution DET gel samples were analysed for ΣNO_3^- in order to pinpoint potentially narrow peaks in concentration.

The concentration of dissolved sulphide in the pore-waters was determined on board using a scaled-down version of the Cline (1969) method (relative standard deviation, RSD < 3%). The remaining conventional pore-water analyses were conducted in the laboratory. Ammonia was analysed using a flow-injection analyser (Hall & Aller 1992) (RSD < 4%). Sulphate and chloride were analysed using a Dionex DX100 ion chromatograph with AS14 column (RSD < 5%). Manganese was analysed using a Perkin-Elmer Zeeman 4100 ZL atomic absorption spectrophotometer (RSD < 5%) and total iron was analysed using a flow-injection analyser (RSD < 5%). ΣNO_3^- (NO_3^- + NO_2^-) determinations for DET gel samples were performed using a small-volume adaptation of the cadmium-copper reduction method (Harris & Mortimer 2002). Previous work demonstrated that ΣNO_3^- peaks can be very sharp, with high concentrations but with limited spatial depth. A conservative approach to interpreting the data was therefore taken in which only points above 50 µM which were supported by at least 1 adjacent elevated value were considered significant. This resulted in the exclusion of 4 DET gel samples from a total of 280 determined.

Nitrification rate measurements. ^{15}N analysis was performed on four 5 cm diameter sub-cores of 12 cm length taken from Box Core 7. A solution of $^{15}NH_4^+$ (ammonium chloride 98% ^{15}N, Sigma-Aldrich) was injected into 2 of the sub-cores via diametrically opposing septa covering the entire depth of the core (12 cm), resulting in a final pore-water concentration of approximately 100 µM $^{15}NH_4^+$ (typical *in situ* concentration; Mortimer et al. 2002). All 4 sub-cores were overlaid with water and incubated in the dark at *in situ* temperatures for 4–6 h. Pore-water was then extracted from 2 cm depth core-slices by centrifugation. Subsamples of the pore-water were preserved with mercuric chloride for analysis of nitrate and nitrite (SKALAR autoanalyser). The nitrate and nitrite in the remainder were reduced to N_2O hydroxylamine according to the method of Stevens & Laughlin (1994). Positive at.% excess $^{15}N_2O$ was used as indicator of nitrification activity and nitrification rates were calculated by producing standard solutions of $^{15}NO_2^-$, and processed as described above to produce calibration curves from which real at.% excesses could be converted into concentrations. The change in % excess during the incubation was then calculated as a change in concentrations over time for a given volume, expressed as nitrification rates. Analysis of $^{15}N_2O$ was undertaken using a 20:20 GC isotope ratio mass spectrometer with an ANCA-TG11 gas preconcentrator. Sediments were only analysed to a sediment depth of 12 cm, as geochemical analysis of the same sampling site in previous studies had indicated pronounced ΣNO_3^- peaks at 10 cm sampling depth.

Molecular analysis of microbial ammonia oxidising communities. ***DNA/RNA extraction and PCR/RT-PCR amplification:*** Sediments were compacted by centrifugation at 13000 rpm for 10 min and excess water removed. Nucleic acids were extracted and purified as described by Griffiths et al. (2000) from 0.5 g of compacted sediment after disruption of cells by bead-beating. DNA and RNA templates were prepared following resuspension of extracted nucleic acids in 50 µl of RNase-free sterile water, and DNA templates were further purified using 0.5 ml Vivaspin concentrator columns (Vivascience. Sartorius). Nucleic acid extracts were quantified by standard agarose electrophoresis and PCR templates were adjusted to equal concentrations by dilution. Ammonia-oxidiser 16S rRNA gene fragments were amplified from extracted DNA by nested PCR using β-proteobacterial ammonia oxidiser primers CTO189f-GC and CTO654r (Kowalchuk et al. 1997) followed by the general eubacterial primers 357f-GC–518r (Muyzer et al. 1993), after a 1:50 dilution to prevent non-specific amplification. Planctomycete 16S rRNA gene fragments were amplified using the semi-specific *Planctomycetales-Verrucomicrobia* (PV) assay (Derakshani et al. 2001) with the primers PLA40f and 1492r. 16S rRNA gene fragments were also amplified from DNA generated from extracted RNA by reverse transcriptase-PCR (RT-PCR) using a modification of the method described by Griffiths et al. (2000). DNA-free RNA was obtained by treating 8 µl of extracted RNA with 2 U of RQ1 RNase-free DNase (Promega) for 30 min at 37°C, to which 8 µl of RT reaction mixture (SuperScript RT RNase H-reverse transcriptase, GibcoBRL) was added according to the manufacturer's instructions. We used 1 µl of digested nucleic acids as PCR-template to ensure complete removal of DNA. Reverse transcription was carried out at 42°C for 50 min and the enzyme was subsequently heat-inactivated for 15 min at 70°C.

PCR-amplified fragments were resolved by standard horizontal electrophoresis on 1% (w/v) agarose gels. 16S rRNA gene fragments were also PCR-amplified from pure cultures and clones representative of β-proteobacterial AOB clusters as described by Stephen et al. (1996) and Webster et al. (2002). *Planctomyces maris* AL (NCIMB 2232) and *P. brasiliensis* VL32 (NCIMB 13185) were used as controls for PCR amplifications with the PV assay. The primers and the PCR conditions for all primer pairs used are summarised in Table 2. Individual reagents and their con-

Table 2. Primers and PCR conditions. GC clamp was attached to the 5′ end of Primers CTO189f and 357f. The general thermocycling programme was 5 min at 94°C; followed by 10 cycles of 30 s at 94°C, 30 s at the specified annealing temperature, and specified extension time at 72°C; followed by 25 cycles of 30 s at 92°C, 30 s at the specified annealing temperature and specified extension time at 72°C (increasing by 1 s cycle^{-1}); followed by a 10 min final extension at 72°C. AOB: ammonia-oxidising bacteria; DGGE: denaturing gradient gel electrophoresis

Primer set (fragment length)	Target group	PCR approach	Thermocycling programme
CTO189f-GC–CTO654r (465 bp)	β-subgroup AOBs	DGGE/nested amplification, 1st stage	Initial denaturing time 5 min; annealing temperature 55°C; extension time 45 s; final extension time 5 min
PLA40f-pf1053r (1.0 kb)	*Planctomycetales-Verrucomicrobia*	DGGE/nested amplification, 1st stage	Initial denaturing time 5 min; annealing temperature 61°C; extension time 70 s
357f-GC–518r (161 bp)	Eubacteria	DGGE/nested amplification, 2nd stage	Initial denaturing time 2 min; annealing temperature 55°C; extension time 30 s; final extension time 5 min

centrations were as follows: 1 × PCR buffer (Bioline), 1 U *Biotaq* DNA polymerase (Bioline) and 1.5 mM $MgCl_2$; each primer had a concentration of 0.2 µM and each deoxynucleoside triphosphate (Bioline) a concentration of 250 µM. Amplification was performed with a total volume of 50 µl, using an Omn-E thermal cycler (Hybaid) and applying the thermal cycle conditions in Table 2.

DGGE and sequence analysis: PCR amplification products were amplified using DGGE as described by Kowalchuk et al. (1997) using 1.5 mm 8% polyacrylamide gels containing denaturing gradients of 40–60% (CTO 189f-GC–CTO654r PCR products) and 35–62% (357f-GC–518r PCR products). Polyacrylamide gels were stained with ethidium bromide. Individual bands from DGGE bands were excised and suspended overnight at 4°C in 30 µl of sterile water to elute DNA. Reamplified PCR products were analysed by DGGE, to ensure purity and correct migration, and sequenced with the 518r primer. Sequencing reactions were performed using the BigDye terminator cycle sequencing kit (PE Biosystems), and the sequencing products were analysed with a Model AB1377 automated sequencer (PE Biosystems). Sequences were aligned using the Sequencer 4.0 programme (Genes Codes Corporation). For phylogenetic analysis, partial nucleotide sequences (160 bp, spanning the hypervariable V3 region of the 16S rDNA) were aligned with closely related 16S rRNA sequences retrieved from the GenBank database at the National Centre for Biotechnology Information (USA) using the basic local alignment search tool (BLASTn). Similarities and mismatches between sequences derived from DGGE-excised bands and sequences retrieved from the GenBank were analysed using the B12Seq algorithm (Altschul et al. 1990).

Phylogenetic relationships between pairs of 16S rDNA sequences were calculated using distance analysis as implemented in PAUP 4.1 (phylogenetic analysis using parsimony). A maximum-likelihood analysis of the most parsimonious trees, constructed from a subset of sequences representing the major sequence groups, was used to estimate the proportion of variable sites needed for the analysis of log/det paralinear distances of variable sites (Lake 1994). Log/det paralinear distances were calculated using the minimal evolution criterion, and data were bootstrapped 1000 times. Phylogenetic trees were constructed from distance analysis using the neighbour-joining method. Established tree topologies were confirmed by repeated analysis with aligned sequence fragments of >1 kb only, excluding the isolated 160b 16S rRNA sequences, and trees were merged.

Nucleotide sequence accession numbers: The partial 16S rDNA sequences determined in this study have been deposited in the GenBank database under Accession Nos. AY156995–AY157006.

RESULTS

Pore-water profiles

Pore-water profiles showed dramatic changes in the concentrations of O_2, ΣNO_3^- (NO_3^- + NO_2^-), Mn^{2+} and Fe^{2+} within the upper ~5 cm of sediment for Cores 8 and 9 (Figs. 2 & 3). Oxygen electrode measurements demonstrated that dissolved oxygen in Core 9 was undetectable at depths greater than 3 mm (Fig. 3). ΣNO_3^- concentrations in overlying Loch Duich seawater determined for both Cores 7 and 9 by DET were approximately 5 µM. A sharp subsurface peak of

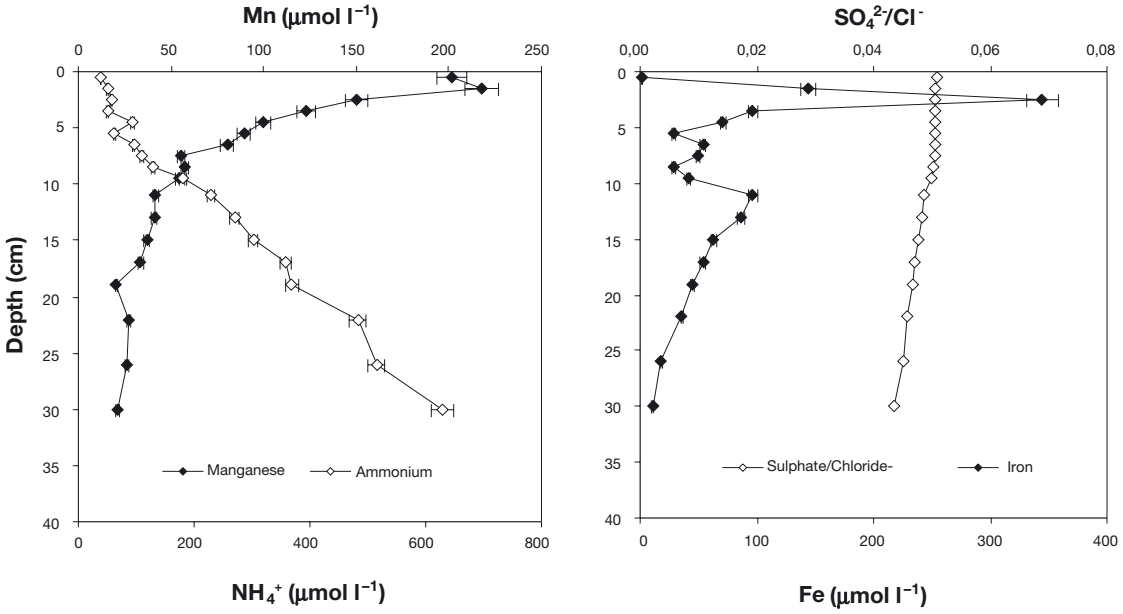

Fig. 2. Pore-water profiles of manganese, ammonium, iron and sulphate/chloride ratio for Core 8, obtained using the conventional slicing and centrifugation method

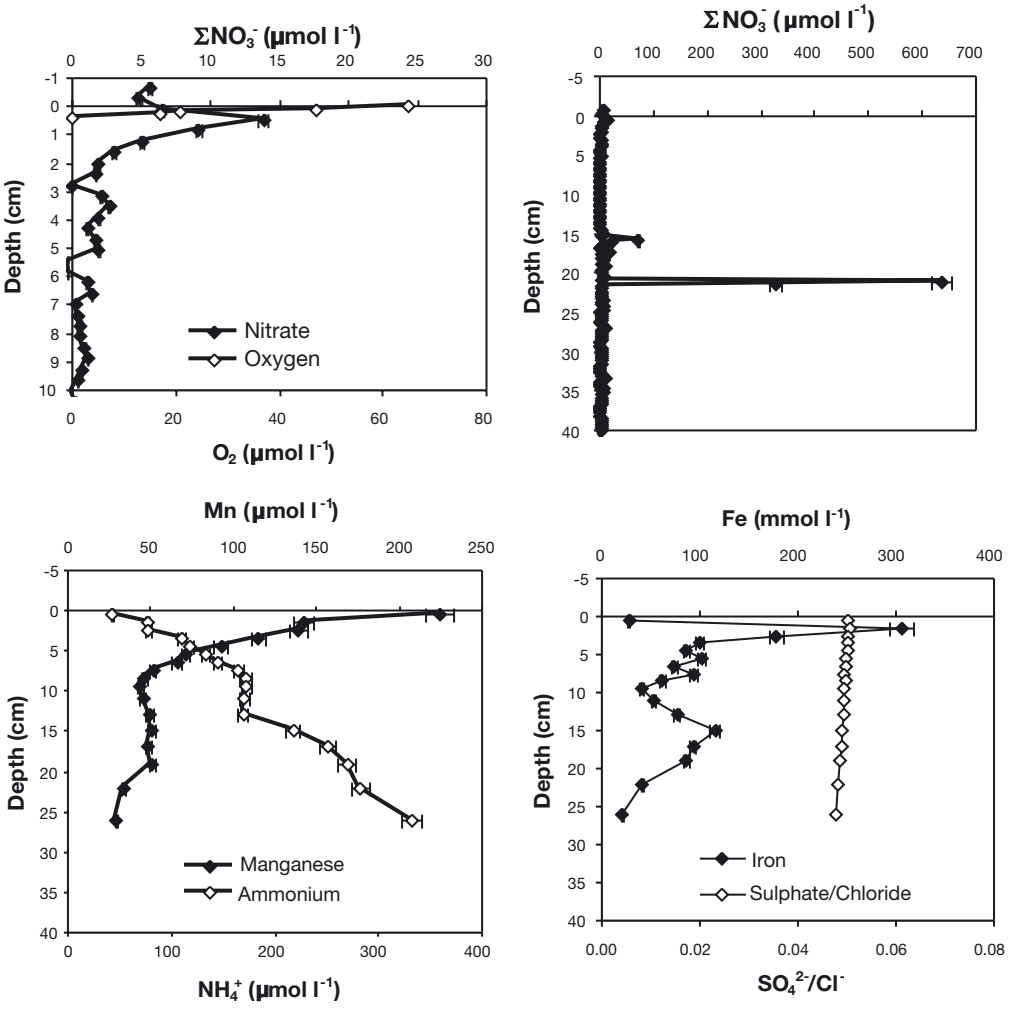

Fig. 3. Pore-water profiles of total nitrate, oxygen, manganese, ammonium, iron and sulphate/chloride ratio for Core 9. Oxygen profile was measured by mini-electrode, total nitrate by DET (diffusive equilibrium in thin films) gel probe, and remaining profiles by conventional slicing and centrifugation method

14 µM ΣNO_3^- was observed in Core 9 at a depth of 5 mm below the sediment-water interface. Deeper subsurface peaks in ΣNO_3^- were also observed in Cores 7 and 9 in regions well below the oxygen penetration depth. A well-defined but small subsurface increase in ΣNO_3^- was observed in Core 7 from 5–8 cm, reaching a maximum concentration of 18 µM (Fig. 4). Core 9 showed an extremely sharp and considerably larger peak of 635 µM ΣNO_3^- at 21 cm below the sediment water interface (Fig. 3). This peak was detected in 2 gel samples spread over a depth interval of ~4 mm.

In Cores 8 and 9, manganese concentrations decreased between the upper 1–2 and 8 cm sediment depth (Figs. 2 & 3). Below 8 cm, manganese concentrations decreased more gradually. Relatively sharp subsurface peaks in iron concentration were also observed in these cores 1.5–2.5 cm below the sediment water interface (Figs. 2 & 3), with broader peaks at 11 and 15 cm depth for Cores 8 and 9 respectively. Although dissolved sulphide was not detected by pore-water analysis over the depth sampled, the sulphate to chloride ratios for Cores 8 and 9 showed significant decreases with increasing sediment depth (Figs. 2 & 3).

Populations of ammonia-oxidising bacteria (AOB)

Total sediment DNA consisted of high-molecular-weight DNA fragments with maximum yields of DNA and RNA in the uppermost sediment layers and decreasing DNA and RNA concentrations with increasing sediment depth (2.5–0.9 µg DNA g^{-1} sediment; 3.5–0.2 µg RNA g^{-1} sediment). PCR amplification specific for β-proteobacterial AOB using the CTO189f-GC–CTO654r primers, and for *Planctomycetes–Verrucomicrobia* using the PV-assay, generated products throughout the entire anoxic region in all analysed cores. PCR amplification signals for β-Subgroup AOB decreased with increasing depth, suggesting a decrease in absolute or relative PCR template copy numbers.

PCR amplification using cDNA templates transcribed from 16S rRNA gene fragments was equally successful and generated high yield products for β-proteobacterial AOB and *Planctomycetes–Verrucomicrobia* throughout the entire anoxic region in all analysed cores.

DGGE analysis of PCR products amplified from DNA using β-proteobacterial AOB primers CTO189f-GC–CTO654r demonstrated 2 dominant bands in all samples (Fig. 5). Co-migration with established reference sequences and excised and sequenced DGGE bands suggested the association of both the upper and lower bands with the *Nitrosospira* Cluster 1 clade. Density analysis of DGGE profiles showed an increase in relative intensity of DGGE bands associated with Sequence LD1-envA2 with increasing depth, and a decrease in relative intensity of DGGE bands associated with all other *Nitrosospira* Cluster 1-associated sequences, suggesting greater relative abundance of LD1-envA2 in deeper sediments (Fig. 6). There was

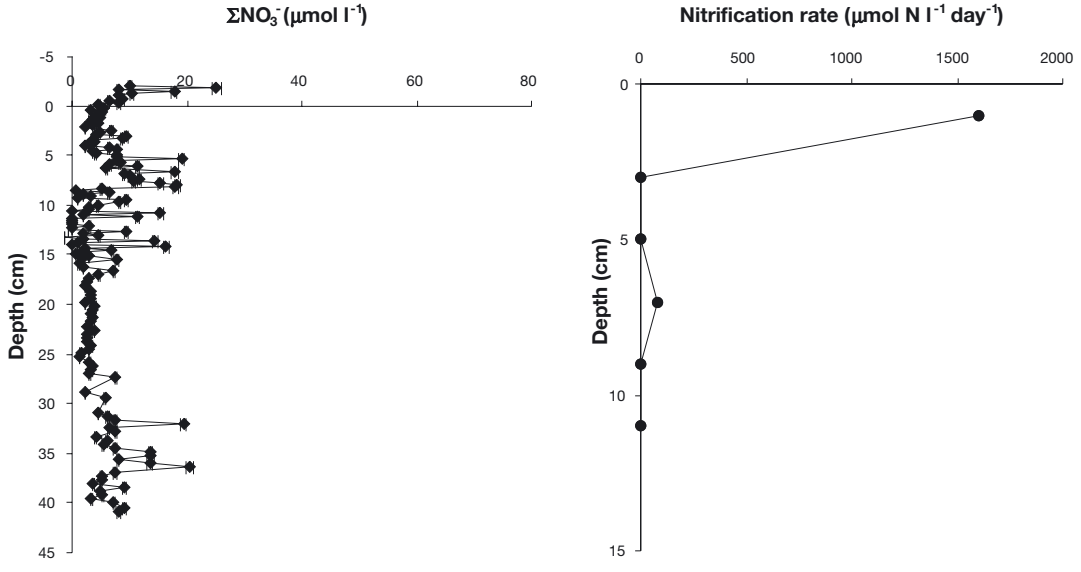

Fig. 4. Pore-water nitrate profile and nitrification rate for Core 7. Total nitrate measured by DET gel probe

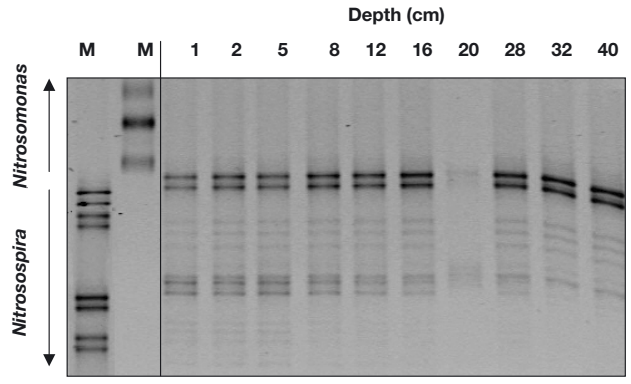

Fig. 5. Denaturing gradient gel electrophoresis (DGGE) analysis of of CTO189f-GC–CTO654r 16S rDNA sequences from Core 8 Loch Duich marine sediments with representative β-proteobacterial ammonia-oxidiser cluster controls. Lane 1 (from bottom to top): EnvB1-8 (*Nitrosospira* Cluster 1); pH7B/C3 (*Nitrosospira* Cluster 4); pH4.2A/27 (*Nitrosospira* Cluster 2); pH4.2A/4 (*Nitrosospira* Cluster 3); Lane 2 (from bottom to top): EnvA1-21 (*Nitrosomonas* Cluster 5); EnvC1-19 (*Nitrosomonas* Cluster 6); *N. europaea* (*Nitrosomonas* Cluster 7). Lanes 3–12: depth profile of Loch Duich Core 8 sediment samples

little other detectable variation in profiles from different cores or depths, suggesting only minor changes in the AOB community composition throughout the anoxic zones of the analysed cores. However, migration patterns of the 465 bp CTO fragments of 16S rDNA PCR products for the 20 cm sample in Core 8 demonstrated a change in the AOB community that was coincident with a peak in ΣNO_3 concentrations in that core.

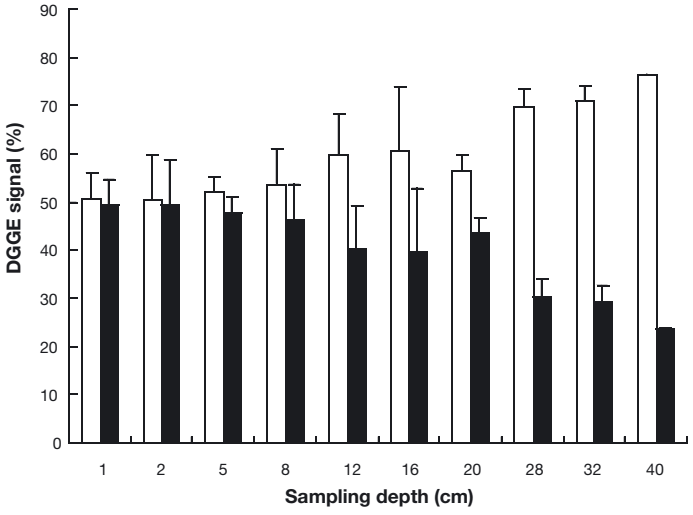

Fig. 6. Average relative abundance of β-proteobacterial ammonia-oxidising bacteria, assessed by PCR amplification of 16S rRNA genes using CTO189f-GC–CTO654r primers, within depth profiles of marine Loch Duich sediments. Ammonia-oxidiser clusters were resolved by DGGE and relative band intensities were quantified by densitometry. Error bars represent standard errors for triplicate sediment samples

Greater discrimination was obtained by DGGE analysis of the nested PCR products (160 bp), generated by first-round amplification using β-proteobacterial AOB primers and second-round amplification using eubacterial primers. This approach indicated highly complex communities, represented by more than 15 individual sequences per sample, throughout the anoxic zones of all cores analysed (Fig. 7). Depth-dependent variation in the intensity of major DGGE bands, indicating changes in relative abundance, were less pronounced than in DGGE profiles of 465 bp fragments, probably due to saturation of PCR templates in the nested PCR approach. The most prominent difference between individual samples was observed for the 20 cm depth in Core 8, which was marked by the absence of 3 dominant bands characteristic of all other samples, and the presence of an additional dominant band.

Separation of 160 bp AOB PCR products generated from 16S rRNA fragments by RT-PCR demonstrated more pronounced differences in the presence and absence of specific bands between individual samples (Fig. 8). An additional prominent band, not observed in DGGE patterns of 16S rDNA profiles, increased in relative intensity with increasing depth in all cores analysed. Depths 14, 18 and 20 cm of Core 8 showed additional prominent bands, which were only observed as faint bands in other samples, indicating higher relative abundance of corresponding 16S rRNA fragments within these samples.

We obtained 8 sequences from excised DGGE bands, but none showed 100% similarity to sequences downloaded as closest matches from GenBank. Phylogenetic analysis of these sequences supports the presence of novel, previously undescribed sequences closely associated with β-proteobacterial AOB within the anoxic Loch Duich sediments (Fig. 9). *Nitrosospira*-like sequences were associated with *Nitrosospira* Cluster 1 clone sequences that isolated from marine environments (Stephen et al. 1996, Kowalchuk et al. 1997, Phillips et al. 1999, Bano & Hollibaugh 2000). *Nitrosomonas*-like sequences were associated with *N. europaea* Cluster 7 and *N. marina* Cluster 6. However, the most prominent *Nitrosomonas*-like sequences could not unambiguously be associated with traditional *Nitrosospira* sp. or *Nitrosomonas* sp., but were associated with the recently proposed *Nitrosomonas* sp. Nm143 lineage (Purkhold et al. 2003).

Co-migration of excised and reamplified DGGE sequences with environmental Loch Duich amplicons demonstrated the *Nitrosospira* Cluster 1-like sequences LD1-env-A2 and LD1-env-A8 as dominant in almost all 16S rDNA amplifications. These sequences were, however, absent from the 20 cm depth, Core 8

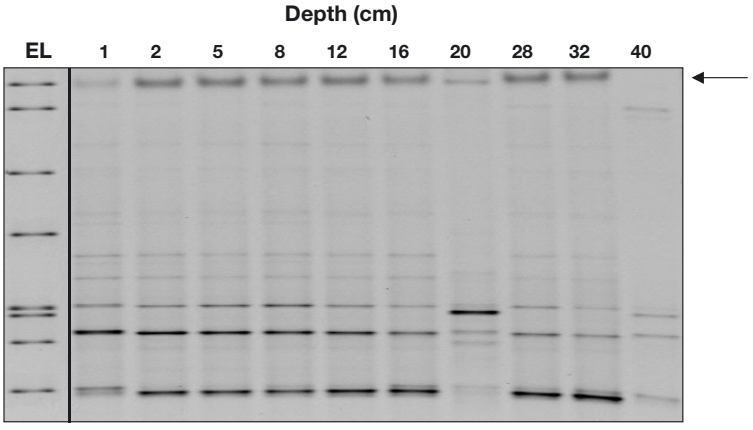

Fig. 7. DGGE analysis of nested 357f-GC–518r 16S rDNA β-proteobacterial ammonia-oxidiser PCR products from Loch Duich marine sediments and reference sequences derived from bands excised from DGGE gels. Lane 1 (EL = environmental library): excised and reamplified DGGE sequences; Lanes 2–14: depth profile of Core 8 Loch Duich sediment samples. DGGE excised sequences shown in Lane 1 are (from top to bottom): LD1-env-A12, LD1-env-B12, LD1-env-B11, LD1-env-B5, LD1-env-A8, LD1-env-A5, LD1-env-A1, and LD1-env-A2. Arrow marks a prominent band for which no sequence could be determined

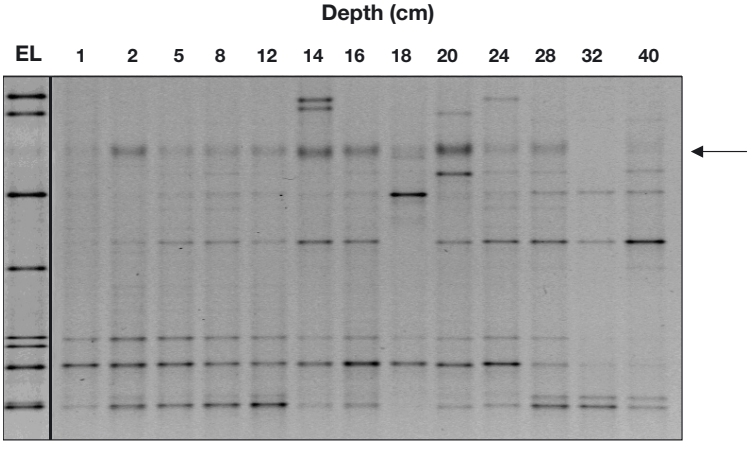

Fig. 8. DGGE analysis of nested 357f-GC–518r 16S rRNA β-proteobacterial ammonia-oxidiser amplicons generated by RT-PCR from Loch Duich marine sediments and reference sequences. Lanes 1–14 and arrow marker as in Fig. 7

sample, but *Nitrosospira* Cluster 1-like sequence LD1-env-A5 was present as the dominant sequence. The marked band in the 16S rRNA amplifications of the 18 cm depth, Core 8, was associated with the *Nitrosomonas* sp. Nm143 lineage and 1 of the prominent bands in 14 cm depth, Core 8 was associated with the *N. marina* Cluster 6.

Separation of 160 bp 16S rDNA PCR products generated with the PV-assay demonstrated highly similar, complex communities of *Planctomycetes-Verrucomicrobia* throughout the anoxic zones of all cores analysed. Differences in DGGE profiles were restricted to the presence or absence of faint bands. Prominent bands indicating higher relative abundance of individual DNA-derived sequences were not detected, but were present in DGGE profiles of 16S rRNA amplicons generated by RT-PCR. Sequences generated from 7 of these bands had no unambiguous match with sequences in GenBank. Alignment and phylogenetic analysis suggested the association of Planctomycetes with Verrucomicrobia, the bacterial candidate lineages WS3 and BRC1 of the isolated sequences. No sequence with an association with recognised anammox sequences was identified.

Nitrification rates: Core 7

Nitrification activity was greatest in the upper 0–2 cm sediment interval (1600 µM l^{-1} d^{-1}. Nitrification was not detected below 2 cm sediment depth, with the exception of a small peak (84 µM l^{-1} d^{-1}) within the sediment interval 6–8 cm (Fig. 4, Table 3).

DISCUSSION

Biogeochemical reaction sequence: Cores 8 and 9

The oxygen penetration depth of 3–4 mm for Core 9 (Fig. 3), is similar to that inferred previously for Loch Duich (Hayes 2001). Below this depth, Sediment Cores 8 and 9 are described as 'anoxic' on the basis that free dissolved oxygen is not detected. The near-surface profile for Core 9 (Fig. 3) clearly shows a maximum in ΣNO_3^- close to the oxic/anoxic boundary. This profile is characteristic of the conventional nitrification/denitrification couple typically found in marine sediments (e.g. Fenchel et al. 1998). Direct evidence for this subsurface conventional nitrification is provided by the ^{15}N rate measurements, with the highest rate determined in the upper 2 cm of the sediments (Fig. 4). The decrease in ΣNO_3^- below 4 mm then reflects denitrification to N_2 gas or a decrease in nitrification alone, although the slight asymmetry to the peak suggests that the former is more likely. The manganese profiles (Figs. 2 & 3) indicate that manganese reduction is predominantly within the upper 5 cm. The iron profiles (Figs. 2 & 3) suggest that iron reduction follows manganese reduction, but the presence of an additional peak at 15–20 cm indicates that

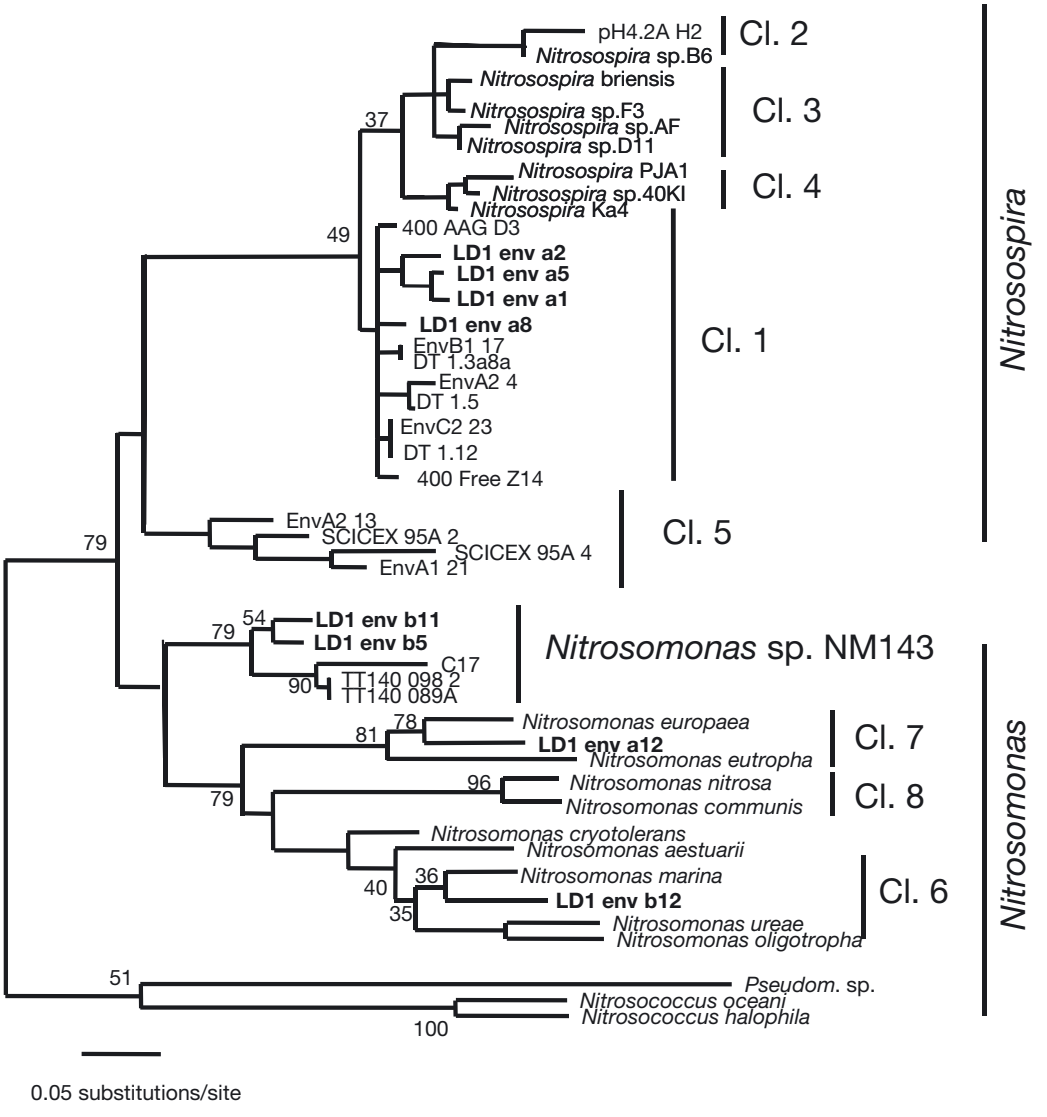

Fig. 9. Evolutionary distance dendrogram showing the positions of environmental 16S rDNA 160 b DGGE sequences (in boldface) recovered from anoxic marine sediments in relation to representative members within β-proteobacterial ammonia-oxidisers. Tree based on results of neighbour-joining analysis of log/det paralinear distances. Multifurcation connects branches for which a relative order could not be determined unambiguously. Scale bar indicates estimated 0.05 changes per nucleotide position

Table 3. ^{15}N nitrification rates (6 h incubation) for cores collected in Loch Duich (July 2000)

Depth (cm)	Oxidised inorganic N recovered (µM)	$^{15}N_2O$ (%)	^{15}N (µM)	Nitrification rate (µM l^{-1} d^{-1})
0–2	13.6	46	6.25	1600
2–4	0.0175	2	0.000350	0.0896
4–6	0.0019	1	0.000019	0.00486
6–8	2.18	15	0.327	83.8
8–10	0.604	1	0.00604	1.55
10–12	0.018	1	0.000180	0.0461

the process is still occurring at depth. Previous sampling of pore-waters at the same site in Loch Duich (Davies 1976, Krom & Sholkovitz 1978, Hayes 2001, Mortimer et al. 2002) showed a distinct boundary at 20–30 cm, below which free sulphide accumulated. It is therefore somewhat unusual that a zone below which free sulphide continues to accumulate was not evident in the pore-water analysis results presented here.

Evidence for anoxic nitrification: DET and molecular analysis

Previous work from Loch Duich showed a large (900 µM) ΣNO_3 peak ~10 cm below the sediment-water interface at a position where both sulphate and dissolved Fe began to decrease (Mortimer & Krom 1998, Mortimer et al. 2002). It was suggested that such peaks are produced be perturbation of previously unrecognised nitrogen recycling processes occurring throughout the anoxic region. Since the ΣNO_3 peak was too sharp to be sustained, it was interpreted as a non-steady-state phenomenon (Mortimer et al. 2002). A similar well-defined high concentration ΣNO_3 peak was found in the study presented here (Core 9, ca. 21 cm, Fig. 3), supporting the hypothesis that large (0.5–1 mM) non-steady-state ΣNO_3 peaks can be a feature of anoxic marine sediments. However, as with previous studies in this system, such ΣNO_3 peaks were not found in all cores taken, and varied in width and concentration. The peak occurred over 2 sampling points (3–4 mm) compared with 6 sampling points (10 mm) found by Mortimer et al. (2002), and was also smaller in maximum concentration (640 compared with 900 µM). Using Fick's 1st law, the mean flux of ΣNO_3 away from the peak is calculated to be ca. 10 mM m^{-2} d^{-1}. Assuming that it is a transient, non-steady-state feature, it would take approximately 13 h for the peak to disappear by diffusion. Conversely, a nitrification rate of ca. 1.2 mM N $l^{-1}d^{-1}$ (approximately 75% of the rate measured at the sediment surface) would be required to maintain such a peak.

Direct amplifications of 16S rDNA and RNA suggest that β-proteobacterial ammonia-oxidising bacteria (AOB) are present throughout the anoxic Loch Duich sediments. DGGE patterns of additional reference samples from the neighbouring Raasay Sound (data not shown), which is a sandier and less organic-rich sediment, demonstrated similar AOB DGGE community patterns, but of lower band intensities, suggesting that the organic-rich Loch Duich sediments favour diverse communities of AOB. However, the uniformity of the DGGE signals generated from amplification of 16S rDNA fragments indicates that the AOB community composition varies little with depth or between sites. The results for the 7 sediment cores analysed suggest that the Loch Duich sediments contain a highly diverse but spatially uniform community of AOB within the upper 40cm anoxic region. Amplification of 16S rDNA fragments alone does not distinguish between active and inactive AOB within the anoxic zone. However, the successful amplification of 16S rRNA gene fragments using RT-PCR suggests that high rRNA levels are maintained throughout the anoxic zone. It has been argued that rRNA levels within β-proteobacterial ammonia-oxidising bacteria may be maintained over considerable periods of time (5 h) and are thus no reliable indicator for rapid metabolic activity (Wagner et al. 1995). In experimental trials however, RT-PCRs on environmental samples stored for several weeks at 4°C failed to generate amplicons, or showed significantly diminished DGGE migration patterns (T. E. Freitag unpubl. data). It can thus be assumed that the anoxic Loch Duich sediments are stable for substantially longer periods and that cells indicated by RT-PCR may be metabolically active.

Shifts in relative proportion of sequences within mixed PCR products indicated by changing DGGE band densities have been used to establish changes in bacterial community composition in numerous studies (e.g. Phillips et al. 1999, Nicol et al. 2003). The increase in the relative abundance of *Nitrosospira* Cluster 1 LD1-envA2 sequences with increasing sampling depth and the increasing signal intensity of corresponding rRNA DGGE bands suggests that they are present in high copy numbers in anoxic sediments, and that the bacteria they represent may be more adapted to reducing geochemical environments than the other detected *Nitrosospira* Cluster 1 sequences or, if the bacteria are inactive or dead, are more resistant to degradation under reducing anoxic conditions. The *Nitrosospira* Cluster 1 LD1-envA2 AOB may thus be at a selective advantage in more reducing environments compared with the other *Nitrosospira* Cluster 1 like AOB that seem to be present in higher copy numbers within the higher sediment layers in Loch Duich. Representatives of *Nitrosospira* Cluster 1-type strains have not been obtained in laboratory culture, making it unwise to speculate on their potential activity, but evidence from other ammonia oxidisers suggest the possibility that they may carry out denitrification in anaerobic sediments.

The position of a major ΣNO_3^- peak at 21 cm depth in Core 9 shows a correlation with the depth at which a shift in AOB community composition was observed in the immediately adjacent Core 8 (Fig. 8; 20 cm). This suggests that changes in the microbial population of β-proteobacterial AOB may be linked to the occurrence of a non steady state ΣNO_3^- peak. It is however unclear (1) why differences in the composition of the microbial population that is otherwise remarkably uniform would exist at 20 cm depth within anoxic sediments, (2) over what time scale such changes in composition could occur, or (3) how differences in composition could be linked to the production of a non-steady-state ΣNO_3 peak. The diversity of DNA- and RNA-derived community profiles suggests AOB populations with spatial differences in community composition and possibly activity. While the sedimentary and geochemical conditions of the Loch Duich sediments may appear to be uniform, slight heterogeneities in the

geochemical profiles and processes may act as the driving forces for the observed shift in community structure and activity of AOB.

It is possible that the large ΣNO_3^- peak could have been produced by macrofaunal burrows or by a sampling artefact. However, other chemical changes consistent with oxygenation by burrows were not seen (cf. Mortimer et al. 1999, 2002). Furthermore, DET gels have been deployed in numerous aquatic environments, yet nitrate peaks remain a feature found only in Loch Duich.

Evidence for anoxic nitrification: DET and ^{15}N nitrification-rate measurements (Core 7)

The well-defined but relatively minor subsurface peak in nitrate detected at ~8 cm below the sediment-water interface in Box Core 7 (Fig. 4) correlates well with the depth of the peak in nitrification rate also found in Core 7. Given that Core 7 was taken from the same sampling station as Cores 8 and 9, the depths at which the peaks in ΣNO_3^- and nitrification rate occur are likely to lie within the anoxic sediments. A possible explanation for this ΣNO_3^- peak and the subsurface peak in nitrification rate is the presence of macrofaunal burrows (cf. Mortimer et al. 1999). However, considering that the sub-cores used to analyse ΣNO_3^- and nitrification were several centimetres apart, it is unlikely that a burrow would have intersected these samples at 7–8 cm depth and not at any other depth. Furthermore, no oxygen was detected at these depths in any cores tested. An alternative explanation for the existence of these peaks at ~8 cm is that they are produced by anoxic nitrification. This is supported by the high ΣNO_3^- concentrations within the anoxic region shown here and previously (Mortimer & Krom 1998, Mortimer et al. 1998, 2002), the anoxic nitrification demonstrated by the ^{15}N measurements, and the successful amplification of 16S rDNA and RNA fragments specific for β-proteobacterial AOB.

Other recent work has suggested that nitrification can occur within anoxic marine sediments (Aller et al. 1998, Hulth et al. 1999, Anschutz et al. 2000, Hyacinthe et al. 2001, Deflandre et al. 2002, Luther & Popp et al. 2002, Mortimer et al. 2002), although the process was found to be insignificant in Mn-rich sediments of the Skaggerak (Thamdrup & Dalsgaard 2000). The continued presence of nitrate at depth in MnO_2-rich Panama Basin sediments led Aller et al. (1998) to suggest anaerobic ammonia oxidation by MnO_2. Anoxic incubations of surface marine sediment showing anoxic nitrate production during Mn reduction were interpreted by Hulth et al. (1999) as evidence for coupled anaerobic nitrification-denitrification. Anschutz et al. (2000) found peaks of nitrate deep within anoxic bioturbated sediments from the Laurentian Trough. The mechanism of anaerobic ammonia oxidation by manganese oxides to produce NO_3^- was suggested on the basis that peaks in Mn^{2+} coincided with the NO_3^- peaks. Further, it was calculated that the anaerobic production of nitrate by reaction of MnO_2 with NH_4^+ is energetically highly favourable whenever Mn (III, IV) oxide minerals are bioturbated into anoxic sediments. It was also concluded by Hyacinthe et al. (2001), based on vertical flux calculations, that a significant proportion of MnO_2 reduction in marine sediments may occur by NH_4^+ oxidation. Deflandre et al. (2002) reported nitrate peaks in anoxic marine fjord sediments coincident with a layer of Mn oxides buried during a flash-flood. Luther & Popp (2002) showed that nitrification of nitrite to nitrate by manganese oxides was also possible, and probably microbially mediated at seawater pH.

Recent experiments involving the incubation of marine sediments taken from within the conventional region of nitrate reduction and amended with ^{15}N-labelled nitrate or ammonium have demonstrated anaerobic nitrate reduction by ammonium (Thamdrup & Dalsgaard 2002). This anaerobic ammonium oxidation was calculated to represent a significant fraction of N_2 production in deep-water marine sediments. The anammox process as described by Jetten et al. (1997), however, is dependent on NO_2^- as terminal electron acceptor for the oxidation of ammonium. Free NO_2^- is generated from NO_3^- by denitrification or by nitrification of ammonium. The anammox process is therefore coupled to processes that are usually associated with the oxic-anoxic interface or, in deeper sediment layers, would be dependent on transport processes like bioirrigation. No anammox-related sequence was isolated from the anoxic Loch Duich sediments, although this may have been due to limitations of the methods used or lower relative abundances. The current knowledge about the physiology of the anammox organism, however, does not support the use of alternative electron acceptors during anoxic ammonia oxidation.

Following the work by Aller et al. (1998), Hulth et al. (1999), Deflandre et al. (2002) and Luther & Popp (2002), a possible mechanism for nitrification in anoxic Loch Duich sediments is that ammonia (or nitrite) oxidation by Mn oxides to produce NO_3^- (Eq. 1 below) (see also Mortimer et al. 2002). Coupled nitrate reduction to N_2 in the anoxic region may then occur via a number of pathways including conventional microbial denitrification using labile organic matter (Eqs. 2–6 below). A fraction of the nitrate flux from anaerobic nitrification may thus be channelled into the reoxidation of Mn^{2+} to produce MnO_2 and N_2 (Eq. 3) (see also

Luther et al. 1997, 1998) to form a coupled nitrification-denitrification reaction (Hulth et al. 1999). This coupling would be consistent with nitrification throughout the anoxic sediments, but with nitrate peaks produced by perturbations in the system disrupting the coupling. Although there is no evidence for a minimum in the ammonium or manganese profiles coincident with the nitrate peak, these would not be expected in the data of Fig. 3, since these profiles were obtained by conventional low-resolution pore-water sampling. In order to fully elucidate the possible interaction between the N and Mn cycles, it would be necessary to measure nitrate, nitrite, ammonia-N and manganese on the same high-resolution DET, because the process only occurs at the microscale. Unfortunately, given the present technology, this is not possible.

Anaerobic nitrification:
Reduction of Mn oxide with ammonia, producing nitrate:

$$8MnOOH + NH_4^+ + 14H^+ \rightarrow 8Mn^{2+} + NO_3^- + 13H_2O$$
$$4MnO_2 + NH_4^+ + 6H^+ \rightarrow 4Mn^{2+} + NO_3^- + 5H_2O \quad (1)$$

Possible coupled denitrification reactions:
Denitrification:

$$5CH_2O + 4NO_3^- + 4\,H^+ \rightarrow 5CO_2 + 2N_2 + 7H_2O \quad (2)$$

Oxidation of Mn^{2+} with nitrate:

$$5Mn^{2+} + 2NO_3^- + 4H_2O \rightarrow 5MnO_2 + N_2 + 8H^+ \quad (3)$$

Oxidation of Fe^{2+} with nitrate:

$$5Fe^{2+} + NO_3^- + 12H_2O \rightarrow 5Fe(OH)_3 + 1/2N_2 + 9H^+ \quad (4)$$

Oxidation of NH_4^+ with nitrite (the 'anammox' process):

$$NO_2^- + NH_4^+ \rightarrow N_2 + 2H_2O \quad (5)$$

Oxidation of sulphide with nitrate:

$$NO_3^- + 5/8FeS + H^+ \rightarrow 1/2N_2 + 5/8SO_4^{2-} + 5/8Fe^{2+} + 1/2H_2O \quad (6)$$

A possible explanation for the non steady-state ΣNO_3 peak is that the rate of reaction (Eq. 1) may be increased due to a locally enhanced concentration of Mn oxides within the sediment. For example, a relict Mn oxide spike at depth in the anoxic zone, caused by a small-scale slumping event, could significantly increase the anoxic nitrification rate (Mortimer et al. 2002). Deflandre et al. (2002) reported similar nitrate peaks in anoxic pore-waters of a marine fjord caused by burial of the surface Mn oxide layer during flash-flood deposition. Loch Duich is extensively trawled, and such activity is known to cause redistribution of sediment on this scale. Furthermore, the sampling site is also within a depression on the Loch floor, and previous ^{14}C measurements have shown the sides to slump (M. D. Krom unpubl. data). Unfortunately, we do not have solid-phase manganese data for the cores sampled herein. However, Fig. 10 shows both dithionite-extractable and total Mn for a core taken nearby (Site LD1, Fig. 1) (Hayes 2001, Krom et al. 2002). Both profiles show a large peak in solid Mn just below the sediment-water interface, but also other peaks much deeper within the sediment. One large peak in total Mn at 18–20 cm depth is mirrored by a peak in the dithionite-extractable Mn, suggesting that labile Mn may be buried to depth within these sediments.

SUMMARY

Anoxic nitrification in organic-rich marine sediments was predicted on the basis of a large non-steady-state ΣNO_3^- peak which had previously been found at depth in anoxic sediments (Mortimer et al. 2002). ΣNO_3^- DET gel profiles again demonstrated the existence of unusually high peaks of ΣNO_3^- at depth within anoxic sediment, well below the presence of any measurable free dissolved oxygen. Analysis of microbial communities of β-proteobacterial AOB by 16S rDNA and 16S rRNA demonstrated a diverse community of AOB that was abundant throughout the anoxic sediment interval analysed. Amplification of 16S rRNA fragments by RT-PCR suggested that a proportion of these AOB may be metabolically active.

A correlation between the depth of the large nitrate peak, a shift in the AOB community composition and the appearance of additional sequences in the 16S rRNA amplifications suggests a link between the occurrence of non-steady-state nitrate peaks, the microbial community composition and activity of ammonia-oxidising bacteria. In particular, the increase in relative abundance of specific β-proteobacterial AOB sequences at 20 cm depth suggests a competitive effect on the AOB communities.

^{15}N microbial rate determinations showed nitrification activity in the upper 1 cm of the sediment coincident with the peak of conventional nitrification. A smaller peak of nitrification activity was observed at ~7–8 cm below the oxygen penetration depth which coincided with a small increase in nitrate and was regarded as evidence of anoxic nitrification activity. However, at other depths within the upper 12 cm sampled, although molecular genetic markers suggested that ammonia-oxidising bacteria were present ^{15}N microbial rate measurements could not detect any measurable nitrification.

The results suggest that anoxic nitrification was occurring throughout the sediment depth sampled, coupled with denitrification. Where this coupling is perturbed, non-steady-state nitrate peaks may result. The source of the oxidant required to support nitrification in the anoxic region is likely to be Mn oxide layers buried during small-scale sediment slumping events.

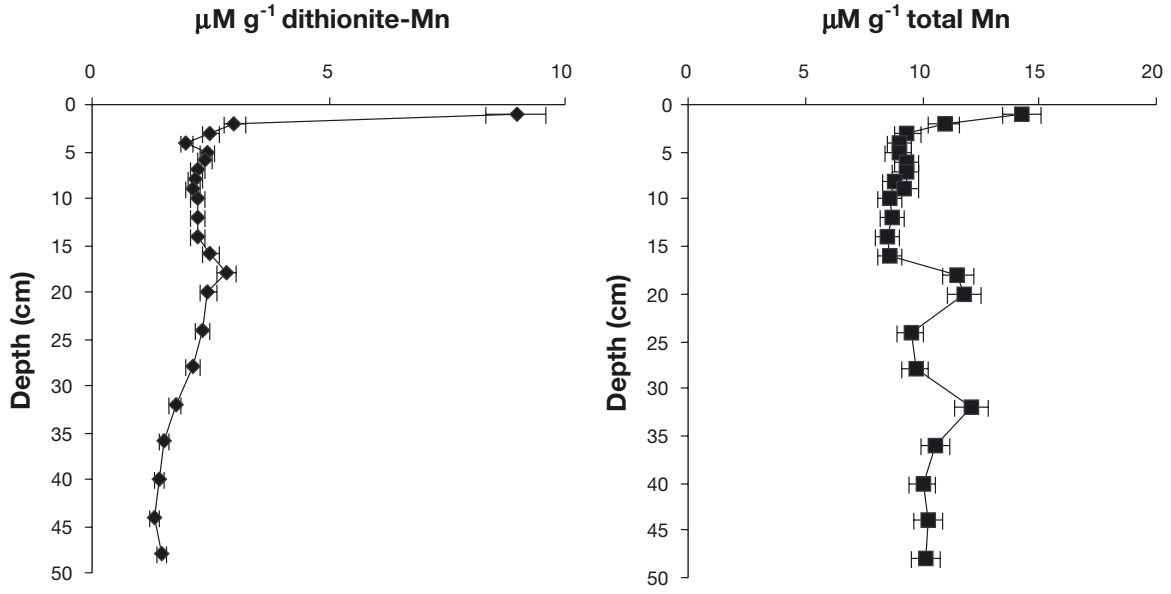

Fig. 10. Vertical profiles of dithionite-extractable and total Mn (HNO3/HCl/HF extraction) for Core LD1, Loch Duich. Mn determined by flame-atomic absorption spectrometry (Perkin Elmer 3300) following standard dithionite or HNO3/HCl/HF extraction (for details see Krom et al. 2002)

The importance of anoxic nitrification in marine sediments remains a matter of debate. Much of the evidence for the process to date has been indirect or incomplete because such a rapid recycling reaction is difficult to measure. Whilst our results point towards the occurrence of anoxic nitrification, further advances in high-resolution pore-water techniques to allow the analysis of ammonium, nitrite, nitrate and dissolved manganese on the same sample are required to detail the process further *in situ.* Only by combining such techniques with similar-resolution solid-phase, molecular and rate measurements can we hope to fully understand N-Mn cycling.

Acknowledgements. We thank the officers and crew of FRV 'Clupea'. This research was supported by Leverhulme Trust Research Grant F/122/BF. The project was completed and the manuscript prepared while M.D.K. was in receipt of a Leverhulme Trust research fellowship (RFG/10307). NERC funded Radiocarbon Dating Allocation 838.1299.

LITERATURE CITED

Aller RC, Hall POJ, Rude PD, Aller JY (1998) Biogeochemical heterogeneity and suboxic diagenesis in hemipelagic sediments of the Panama Basin. Deep-Sea Res I 45: 133–165

Altschul SF, Gish W, Miller E, Myers EW, Lipman DJ (1990) Basic local alignment search tool. J Mol Biol 215**:** 403–410

Anschutz P, Sundby B, Lefrancois L, Luther GW, Mucci A (2000) Interactions between metal oxides and species of nitrogen and iodine in bioturbated marine sediments. Geochim Cosmochim Acta 64:2751–2763

Bano N, Hollibaugh JT (2000) Diversity and distribution of DNA sequences with affinity to ammonia-oxidising bacteria of the β-subdivision of the class *Proteobacteria* in the Arctic Ocean. Appl Environ Microbiol 66:1960–1969

Brendel PJ, Luther GW III (1995) Development of a gold amalgam voltammetric microelectrode for the determination of dissolved Fe, Mn, O_2, and S(-II) in porewaters of marine and freshwater sediments. Environ Sci Technol 29: 751–761

Cline JD (1969) Spectrophotometric determination of hydrogen sulfide in natural waters. Limnol Oceanogr 14: 454–458

Dalsgaard T, Canfield DE, Petersen J, Thamdrup B, Acuna-Gonzalez J (2003) N_2 production by the anammox reaction in the anoxic water column of Golfo Dulce, Costa Rica. Nature 422:606–608

Davies IM (1976) Chemical processes in coastal sediments. PhD thesis, University of Edinburgh

Davison W, Zhang H, Grime GW (1994) Performance characteristics of gel probes used for measuring pore-waters. Environ Sci Technol 28:1623–1632

Deflandre B, Mucci A, Gagne JP, Guignard C, Sundby B (2002) Early diagenetic processes in coastal marine sediments disturbed by a catastrophic sedimentation event. Geochim Cosmochim Acta 66:2547–2558

Derakshani M, Lukow T, Liesack W (2001) Novel bacterial lineages at the (sub) division level as detected by signature nucleotide-targeted recovery of 16S rRNA genes from bulk soil and rice roots of flooded rice microcosms. Appl Environ Microbiol 67:623-631

Fenchel T, King GM, Blackburn TH (1998) Bacterial biogeochemistry: the ecophysiology of mineral cycling. Academic Press, San Diego

Froelich PN, Klinkhammer GP, Bender ML, Luedtke NA and 6 others (1979) Early oxidation of organic matter in pelagic sediments of the Eastern Equatorial Atlantic: suboxic diagenesis. Geochim Cosmochim Acta 43:1075–1090

Griffiths RI, Whiteley AS, O'Donnell AG, Bailey MJ (2000) Rapid method for coextraction of DNA and RNA from nat-

ural environments for analysis of ribosomal DNA- and RNA-based microbial community composition. Appl Environ Microbiol 66:5488–5491

Hall POJ, Aller RC (1992) Rapid, small volume flow injection analysis for ECO_2 and NH_4^+ in marine and freshwaters. Limnol Oceanogr 37:1113–1119

Harris SJ, Mortimer RJG (2002) Determination of nitrate in small volume samples (100 µl) by the cadmium-copper reduction method: a manual technique with application to the interstitial waters of marine sediments. Int J Environ Anal Chem 82:369–376

Hayes P (2001) Diagenetic processes and metal mobilisation in an organic rich Scottish fjord. Department of Earth Sciences, University of Leeds, Leeds

Hulth S, Aller RC, Glibert F (1999) Coupled anoxic nitrification/manganese reduction in marine sediments. Geochim Cosmochim Acta 63:49–66

Hyacinthe C, Anschutz P, Carbonel P, Jouanneau JM, Jorissen FJ (2001) Early diagenetic processes in the muddy sediments of the Bay of Biscay. Mar Geol 177:111–128

Jetten MSM, Logemann S, Muyzer G, Robertson LA, deVries S, van Loosdrecht MCM, Kuenen JG (1997) Novel principles in the microbial conversion of nitrogen compounds. Antonie Leeuwenhoek 71:75–93

Kowalchuk GA, Stephen JR, DeBoer, W, Prosser JI, Embley TM, Woldendorp JW (1997) Analysis of ammonia-oxidising bacteria of the beta subdivision of the class Proteobacteria in coastal sand dunes by denaturing gradient gel electrophoresis and sequencing of PCR-amplified 16S ribosomal DNA fragments. Appl Environ Microbiol 63: 1489–1497

Kowalchuk GA, Naoumenko ZS, Derikx PJL, Felske A, Stephen JR, Arkhipchenko IA (1999) Molecular analysis of ammonia-oxidising bacteria of the β-subdivision of the class *Proteobacteria* in compost and composted materials. Appl Environ Microbiol 65:396–403

Krom MD, Sholkovitz ER (1978) On the association of iron and manganese with organic matter in anoxic marine porewaters. Geochim Cosmochim Acta 42:607–611

Krom MD, Davison P, Zhang H, Davison W (1994) High resolution pore-water sampling with a gel sampler. Limnol Oceanogr 39:1967–1973

Krom MD, Mortimer RJG, Poulton SW, Hayes P, Davies IM, Davison W, Zhang H (2002) In-situ determination of dissolved iron production in recent marine sediments. Aquat Sci 64:282–291

Kuypers MMM, Sliekers AO, Lavik, G, Schmid M and 5 others (2003) Anaerobic ammonium oxidation by anammox bacteria in the Black Sea. Nature 422:608–611

Lake JA (1994) Reconstructing evolutionary trees from DNA and protein sequences: paralinear distances. Proc Natl Acad Sci USA 91:1455–1459

Luther GW III, Popp J (2002) Kinetics of the abiotic reduction of polymeric manganese dioxide by nitrite: an anaerobic nitrification reaction. Aquat Geochem 8:15–36

Luther GW III, Sundby B, Lewis BL, Brendel PJ, Silverberg N (1997) Interactions of manganese with the nitrogen cycle: alternative pathways to dinitrogen. Geochim Cosmochim Acta 61:4043–4052

Luther GW III, Brendel PJ, Lewis BL, Sundby B, Lefrancois L, Silverberg N, Nuzzio DB (1998) Simultaneous measurement of O-2, Mn, Fe, I-, and S(-II) in marine pore-waters with a solid-state voltammetric microelectrode. Limnol Oceanogr 43:325–333

Mortimer RJG, Krom MD (1998) New insights into biogeochemical processes from DET gel probes. Mineralogical Mag NY 62A: 1028–1029

Mortimer RJG, Krom MD, Hall POJ, Hulth S, Stahl H (1998) Use of gel probes for the determination of high resolution solute distributions in marine and estuarine pore-waters. Mar Chem 63:119–129

Mortimer RJG, Davey JT, Krom MD, Watson PG, Frickers PE, Clifton RC (1999) The effect of macrofauna on pore-water profiles and nutrient fluxes in the intertidal zone of the Humber Estuary. Estuar Coast Shelf Sci 48:683–699

Mortimer RJG, Krom MD, Harris SJ, Hayes PJ, Davies IM, Davison W, Zhang H (2002) Evidence for suboxic nitrification in recent marine sediments. Mar Ecol Prog Ser 236: 31–35

Muyzer GE, Dewaal EC, Uitterlinden AG (1993) Profiling of complex microbial-populations by denaturing gradient gel-electrophoresis analysis of polymerase chain reaction-amplified genes coding for 16S ribosomal-RNA. Appl Environ Microbiol 59:695–700

Nicol GW, Glover LA, Prosser JI (2003) The impact of grassland management on archaeal community structure in upland pasture rhizosphere soil. Environ Microbiol 5: 152–162

Phillips CJ, Smith Z, Embley TM, Prosser JI (1999) Phylogenetic differences between particle-associated and planktonic β-proteobacteria ammonia oxidising bacteria in the North Western Mediterranean Sea. Appl Environ Microbiol 65:779–786

Purkhold U, Wagner M, Timmermann G, Pommerening-Röser A, Koops HP (2003) 16S rRNA and amoA-based phylogeny of 12 novel betaproteobacterial ammonia-oxidising isolates: extension of the dataset and proposal of a new lineage within the nitrosomonads. Int J Syst Evol Microbiol 53:1485–1494

Revsbech NP (1983) In-situ measurements of oxygen profiles of sediments by use of oxygen microelectrodes. In: Forstner G (ed) Polarographic oxygen sensors, Springer-Verlag, Berlin, p 265–273

Schmidt I, Bock E (1997) Anaerobic ammonia oxidation with nitrogen dioxide by *Nitrosomonas eutropha*. Arch Microbiol 167:106–111

Schmidt I, Bock E (1998) Anaerobic ammonia oxidation by cell-free extracts of *Nitrosomonas eutropha*. Antonie Leeuwenhoek 73:271–278

Stephen JR, McCaig AE, Smith Z, Prosser JI, Embley TM (1996) Molecular diversity of soil and marine 16S rRNA gene sequences related to beta-subgroup ammonia-oxidising bacteria. Appl Environ Microbiol 62:4147–4154

Stevens RJ, Laughlin RJ (1994) Determining nitrogen-15 in nitrite or nitrate by producing nitrous oxide. Soil Sci Soc Am J 58:1108–1116

Thamdrup B, Dalsgaard T (2000) The fate of ammonium in anoxic manganese oxide-rich marine sediment. Geochim Cosmochim Acta 64:4157–4164

Thamdrup B, Dalsgaard T (2002) Production of N_2 through anaerobic oxidation coupled to nitrate reduction in marine sediments. Appl Environ Microbiol 68:1312–1318

Wagner M, Rath G, Amann R, Koops HP, Schleifer KH (1995) *In-situ* identification of ammonia-oxidising bacteria. Syst Appl Microbiol 18:251–264

Warrington R (1878) On nitrification. J Chem Soc 33:44–51

Webster G, Embley TM, Prosser JI (2002) Grassland management regimes reduce small-scale heterogeneity and species diversity of β-proteobacterial ammonia oxidiser populations. Appl Environ Microbiol 68:20–30

Winogradsky S (1891) Recherches sur les organismes de la nitrification. Ann Inst Pasteur (Paris) 5:577–516

Editorial responsibility: Otto Kinne (Editor), Oldendorf/Luhe, Germany

Submitted: October 23, 2003; Accepted: April 27, 2004
Proofs received from author(s): July 9, 2004